ChemCatChem
Research Article
doi.org/10.1002/cctc.202400270
Chemistry Europe
European Chemical Societies Publishing
www.chemcatchem.org

A Non-Macrocycle Thiolate-Based Cobalt Catalystfor Selective O_2 Reduction into H_2O

Lili Sun,[a] Javier Gutierrez,[a] Alan Le Goff,[a] David Gatineau,[a] Timothy A. Jackson,[b] Marcello Gennari,*[a] and Carole Duboc*[a]

The reduction of dioxygen to produce selectively H_2O_2 or H_2O is crucial in various fields. While platinum-based materials excel in $4H^+/4e^-$ oxygen reduction reaction (ORR) catalysis, cost and resource limitations drive the search for cost-effective and abundant transition metal catalysts. It is thus of great importance to understand how the selectivity and efficiency of 3d-metal ORR catalysts can be tuned. In this context, we report on a Co complex supported by a bisthiolate N2S2-donor ligand acting as a homogeneous ORR catalyst in acetonitrile solutions both in the presence of a one-electron reducing agent (selectivity for H_2O of 93% and TOFi = 3 000 h^{-1}) and under electrochemically-assisted conditions (0.81 V $< \eta <$ 1.10 V, selectivity for H_2O between 85% and 95%). Interestingly, such a predominant $4H^+/4e^-$ pathway for Co-based ORR catalysts is rare, highlighting the key role of the thiolate donor ligand. Besides, the selectivity of this Co catalyst under chemical ORR conditions is inverse with respect to the Mn and Fe catalysts supported by the same ligand, which evidences the impact of the nature of the metal ion on the ORR selectivity.

■■Dear author, please add academic title. Prof., Dr. etc.■■

Introduction

The reduction of dioxygen to produce hydrogen peroxide or water is of vital importance in a variety of fields, including energy storage technology, the study of biological systems, and the exploration of new oxidative chemical reactions involving reactive oxygen species. The development of efficient and selective catalytic systems for oxygen reduction reactions (ORR) is thus essential: the $2H^+/2e^-$ product, H_2O_2, serves as an important chemical oxidant,[1] while the $4H^+/4e^-$ reduction yielding H_2O, plays a key role in the cathode of fuel-cells.[2] For the latter application, platinum-based materials have shown outstanding catalytic performance, but limitations in cost and resources have prompted a significant shift toward the search for cost-effective and abundant transition metal catalysts.

Understanding the reactivity of metal complexes with O_2 largely depends on the nature of the transition metal ion, as well as the electronic and steric features of the supporting ligand, and on second coordination sphere effects. However, figuring out how these various factors precisely dictate the ORR catalytic efficiency and selectivity remains a complex challenge, still requiring intense research to fine-tune selectivity while maintaining optimum performance.

In this field, cobalt complexes have garnered attention for their capability in catalyzing O_2 reduction. While extensive studies have focused on N4-macrocyclic Co-complexes, generally known for promoting selective $2H^+/2e^-$ ORR, research on Co-catalysts with non-macrocyclic ligands remains limited. Among the few examples reported, the use of non-macrocycle ligands has enabled the development of Co-based ORR catalysts exhibiting selectivity for the $4H^+/4e^-$ process.[3] It has also been shown that by tailoring the ligand within the second coordination sphere, selectivity can be directed either towards the $4H^+/4e^-$ or $2H^+/2e^-$ process while preserving high-performance rivaling with the most efficient molecular ORR catalysts.[4] According to mechanistic studies performed with these non-macrocycle Co systems, the selectivity has been proposed to depend on the protonation site of the Co^{III}-hydroperoxide intermediate. Protonation at the distal O triggers the $4H^+/4e^-$ process, while protonation at the proximal O leads to the production of H_2O_2.[4b,5] Non-macrocycle cobalt dinuclear complexes have also been designed to enhance ORR performance by exploiting the synergistic effects between the two metal sites.[6] In the special case of a hexanuclear Co-catalyst, it was also demonstrated that the selectivity can be tuned by changing the temperature.[7]

Most of these Co-complexes are supported by N- and O-donor ligands with modified polypyridine or bipyridine scaffolds. Conversely, a few thiolate-based cobalt complexes have been reported for their reactivity in O_2 activation, but none have been studied for ORR catalysis.[8] These investigations highlighted how thiolate functions are not prone to be oxygenated, even in the presence of highly reactive oxygen intermediates.[9] Moreover, in the case of a Co-macrocycle with thioether donors, it was recently demonstrated that sulfur can be directly involved in the O_2 activation mechanism, acting in synergy with the metal center to stabilize a peroxo moiety.[10]

[a] L. Sun, J. Gutierrez, A. L. Goff, D. Gatineau, M. Gennari, C. Duboc
Univ. Grenoble Alpes, CNRS UMR 5250, DCM, F-38000 Grenoble, France
E-mail: carole.duboc@univ-grenoble-alpes.fr
■■email missing■■

[b] T. A. Jackson
The University of Kansas, Department of Chemistry and Center for Environmentally Beneficial Catalysis, Lawrence, Kansas 66045, United States

Supporting information for this article is available on the WWW under https://doi.org/10.1002/cctc.202400270

In this context, we report here on the first thiolate-supported cobalt ORR catalyst. This complex[11] displays selective $4H^+/4e^-$ ORR activity, either in the presence of a chemical reducing agent or under electro-assisted conditions. Its performance is discussed and compared with other reported Co-based ORR catalysts and also with its Mn and Fe congeners[12] allowing us to evaluate the impact of the nature of the metal on the ORR activity.

Results and Discussion

Solution and redox properties of the pre-catalyst. Our objective was to investigate the previously described dinuclear Co^{II} disulfide complex, $\mathbf{Co_2^{SS}}$ (Scheme 1),[11] supported by the disulfide form (L^{SS2-}) of the N2S2 ligand L^{2-} (L^{2-} = 2,2′-bipyridine-6,6′-diyl(bis(1,1-diphenylethanethiolate), as an ORR pre-catalyst in MeCN solution. $\mathbf{Co_2^{SS}}$ is the oxidized and O_2-stable form of the mononuclear Co^{II} bisthiolate compound **Co** (Scheme 1).[13] While in our previous study, $\mathbf{Co_2^{SS}}$ was identified as the only stable form of the complex in CH_2Cl_2 solution, the situation is different in MeCN as suggested by UV-vis and cyclic voltammetry (CV) data.

The UV-vis spectrum of $\mathbf{Co_2^{SS}}$ in MeCN (Figure S1) displays one weak transition at 818 nm ($\varepsilon = 850\ cm^{-1}M^{-1}$), one in the 625–700 nm region ($\varepsilon = 1900\ cm^{-1}M^{-1}$), together with a more intense band at 447 nm ($\varepsilon = 7000\ cm^{-1}M^{-1}$). These features are not present in the previously reported featureless spectrum of $\mathbf{Co_2^{SS}}$ in CH_2Cl_2, and are similar to those observed for the [Co^{III}LCl] adduct.[11] This is consistent with the fact that, in MeCN solution, the Co^{II} disulfide complex $\mathbf{Co_2^{SS}}$ is in equilibrium with a mononuclear Co^{III}-thiolate $[Co^{III}L(MeCN)]^+$ form ($\mathbf{Co^{MeCN}}$, Scheme 1). A similar equilibrium was previously observed in the case of the homologous iron complexes.[14]

The hypothesis of an equilibrium between $\mathbf{Co_2^{SS}}$ and $\mathbf{Co^{MeCN}}$ has been confirmed by analyzing the redox properties of $\mathbf{Co_2^{SS}}$ in MeCN. The CV (inset of Figure 1) displays two irreversible cathodic processes observed at Epc1 = −0.39 V vs. Fc^+/Fc and Ep_{c2} = −0.60 V (Ep_{a1} = −0.49 V, Ep_{a2} = −0.14 V). While the system at Ep_{c2} can be attributed to the reduction of the disulfide bridge of $\mathbf{Co_2^{SS}}$, as previously observed in CH_2Cl_2 at Ep_c = −0.74 V (Ep_a = −0.10 V), the system at Ep_{c1} can be attributed to the reduction of the mononuclear $\mathbf{Co^{MeCN}}$ complex.

Chemical ORR catalysis. The ability of $\mathbf{Co_2^{SS}}$/$\mathbf{Co^{MeCN}}$ (hereafter referred to as $\mathbf{Co_2^{SS}}$ for simplicity) to catalyze the ORR process was evaluated under homogeneous conditions in MeCN using 2,6-lutidinium tetrafluoroborate acid (LutHBF$_4$, pKa = 14.1 in CH_3CN)[15] as a proton source and octamethylferrocene (Me_8Fc) as the electron source. Me_8Fc ($E_{1/2}$ = −0.41 V vs. Fc^+/Fc) was chosen as a monoelectronic reductant based on the redox properties of $\mathbf{Co_2^{SS}}$ (Epc = −0.38 V vs. Fc^+/Fc in MeCN), to generate *in situ* the O_2-reactive species **Co** (Scheme 1). However, in the presence of $LutH^+$, **Co** is protonated to generate $\mathbf{Co^{SH}}$, as observed by UV-vis and mass spectrometry (Figures S1 and S2).

The catalytic ORR activity was estimated by UV-vis monitoring based on the formation of Me_8Fc^+ (λ_{max} = 750 nm, ε = 420 $M^{-1}cm^{-1}$) resulting from the oxidation of Me_8Fc via equations 1 & 2, depending on whether the process leads to the production of hydrogen peroxide or water, respectively.

$$O_2 + 2\ Me_8Fc + 2\ LutH^+ \rightarrow H_2O_2 + 2\ Me_8Fc^+ + 2\ Lut \quad (1)$$

$$O_2 + 4\ Me_8Fc + 4\ LutH^+ \rightarrow H_2O + 4\ Me_8Fc^+ + 4\ Lut \quad (2)$$

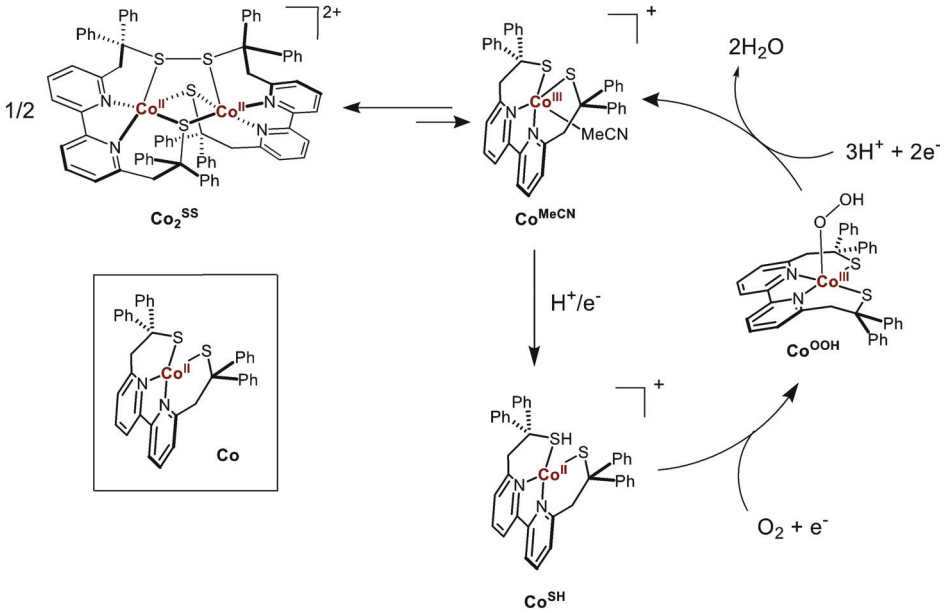

Scheme 1. ORR-related reactivity of the thiolate-supported Co complexes discussed in this paper, including the formation of the hydroperoxo intermediate $\mathbf{Co^{OOH}}$ along with the proposed dominant $4e^-/4H^+$ ORR catalytic pathway.

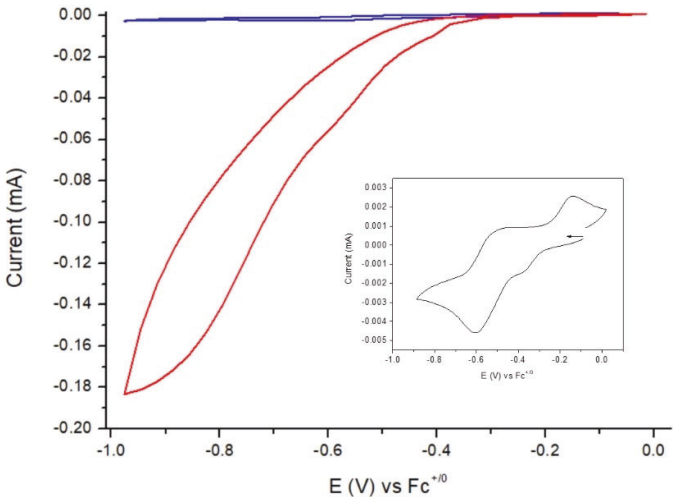

Figure 1. Cyclic voltammograms (CV) of a buffered $LutH^+$/Lut MeCN solution (15.0 mM $LutH^+$ + 15.0 mM Lut) in the absence (blue line) or presence (red line) of 0.1 mM $\mathbf{Co_2^{SS}}$ under an oxygen-saturated atmosphere. Inset: Cyclic voltammogram (CV) of $\mathbf{Co_2^{SS}}$ (0.2 mM) in MeCN under argon-saturated atmosphere. Supporting electrolyte: 0.1 M *n*-Bu_4NPF_4 in MeCN, GC (3 mm diameter) as working electrode, scan rate: 100 mV•s^{-1}.

When $\mathbf{Co_2^{SS}}$ is added in a catalytic amount (0.1 mM) to an air-saturated MeCN solution (~1.6 mM atm^{-1} O_2) that already contains Me_8Fc (2 mM, 20 equiv.) and $LutH^+$ (15 mM, 150 equiv.), the rapid formation of Me_8Fc^+ is observed (Figure 2). In less than 70 s, the catalysis is over with a 96(±3)% yield of Me_8Fc^+ with respect to the initial amount of Me_8Fc. Without a catalyst, Me_8Fc is not oxidized by O_2 within 10 min. Regarding the stability of the $\mathbf{Co_2^{SS}}$ under catalytic conditions, we conducted experiments where 20 equiv. of Me_8Fc were reintroduced at 20 s, 100 s, and 500 s (Figure S6). In each case, we observed a quasi-quantitative Me_8Fc^+ production, as determined in the previous experiment, evidencing the stability of $\mathbf{Co_2^{SS}}$ without degradation after one catalytic run.

The ORR selectivity was investigated by quantifying the amount of H_2O_2 generated during the process based on a spectrophotometric assay using the Ti-TPyP reagent for titration. After 10 min of catalysis in the presence of $\mathbf{Co_2^{SS}}$, only traces of H_2O_2 are detected (Figure S5), in agreement with a selectivity of the catalytic process toward H_2O production (93%, Table S1). The kinetics of the reaction is notably fast, with TOFi = 3(±0.5)×10^3 h^{-1} (= 11(±2) s^{-1}). When the same quantification is performed after 20 s of reaction, H_2O_2 is detected with a selectivity of 25% at this shorter timescale (Table S1), suggesting that some H_2O is formed by a 2 + 2 mechanism.[16] To investigate the hypothesis that a $2H^+/2e^- + 2H^+/2e$ pathway can be involved, experiments were performed with H_2O_2 as the substrate under anaerobic conditions. In the presence of $\mathbf{Co_2^{SS}}$, reduction of H_2O_2 into H_2O is observed with an H_2O_2 conversion of 48% after 10 min, as determined from the quantification of the produced Me_8Fc^+. This is consistent with two pathways for the production of H_2O, the main and fast $4H^+/4e^-$ ORR path (predominant in the first 20 s) and a slower (a few min timescale) competitive stepwise $2H^+/2e^- + 2H^+/2e^-$ mechanism.[16]

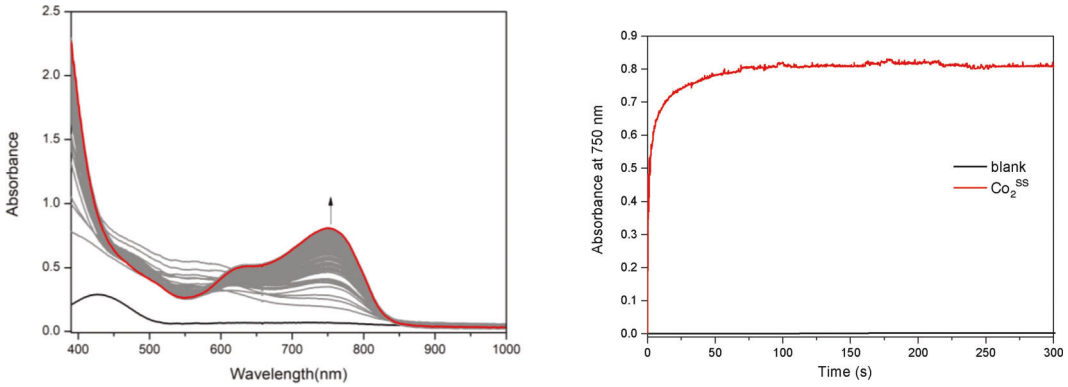

Figure 2. (left) UV − vis spectral changes observed during O_2 reduction catalyzed by $\mathbf{Co_2^{SS}}$ (0.1 mM) in the presence of $LutH^+$ (15 mM) and Me_8Fc (2 mM) in MeCN at 293 K (air-saturated solution, 1 cm path length, Δt = 1 s). (right) The time profiles for Me_8Fc^+ formation (absorbance at 750 nm) in the presence of $\mathbf{Co_2^{SS}}$ (red line) and the corresponding blank sample (no catalyst, black line) are shown.

Electrochemically-assisted ORR catalysis. The promising catalytic ORR properties of $\mathbf{Co_2}^{\mathbf{SS}}$ under chemical conditions prompted us to evaluate its electrocatalytic performance and selectivity under comparable homogeneous conditions. The comparison of the CVs recorded on an oxygen-saturated buffered $LutH^+$/Lut MeCN solution in the absence and presence of $\mathbf{Co_2}^{\mathbf{SS}}$ evidences the appearance of a catalytic process with an onset at ~−0.40 V vs Fc^+/Fc after the addition of the Co complex, attributed to an electrochemical-assisted ORR activity (Figure 1). This is consistent with the fact that the ORR catalysis is initiated by the reduction of the Co^{III}-thiolate MeCN adduct $\mathbf{Co}^{\mathbf{MeCN}}$, which is reduced at a similar potential ($Ep_c = -0.39$ V vs Fc^+/Fc).

The selectivity of the process was investigated through rotating ring-disk electrode voltammetry (RRDE) experiments that enable the quantification of H_2O_2 generated under electrochemical conditions at the Pt ring (potential fixed at 0.2 V vs Fc^+/Fc (Figure 3). An electrocatalytic wave is observed in the presence of O_2 and $LutH^+$/Lut at a mid-wave potential of $E_{cat/2} = -0.42$ V vs Fc^+/Fc. This is close to the $Co^{III/II}$ reduction potential of the MeCN adduct $\mathbf{Co}^{\mathbf{MeCN}}$, confirming its role as the catalytic intermediate again. A Tafel slope of 112 mV dec^{-1} was estimated from the plot of the logarithm of current density versus overpotential, in line with the theoretical value of 118 mV dec^{-1} for rate-limiting single-electron transfer. The % of H_2O_2 quantified at the ring disk at 0.50 V vs. Fc^+/Fc is 22%, corresponding to 3.5 electrons. This aligns with the selectivity measured with a chemical-reducing agent with a predominant $4H^+/4e^-$ ORR pathway. Besides, we can propose that under these electrochemically assisted conditions, the generated H_2O_2 is detected before it can be reduced through the proposed slowest $2H^+/2e^- + 2H^+/2e^-$ path observed under chemical conditions.

From the recorded CVs, the overpotential for the predominant $4H^+/4e^-$ O_2 reduction process can be estimated. The standard overpotential for O_2 reduction in a buffered $LutH^+$/Lut CH_3CN solution is estimated to be E^0 (O_2/H_2O) ≈ 0.39 V or 0.68 V vs Fc^+/Fc depending on the method.[12a] Therefore, with a mid-wave potential of the catalytic wave observed at $E_{cat/2} = -0.42$ V vs Fc^+/Fc, an overpotential between 0.81 V < η < 1.10 V for a $4H^+/4e^-$ O_2 reduction process is determined. The Ep_c ($Co^{III/II}$) value for the $\mathbf{Co}^{\mathbf{MeCN}}$ ORR pre-catalyst (−0.39 V vs Fc^+/Fc, corresponding to +0.10 V vs Fc^{*+}/Fc*), falls within a comparable range to the $E_{1/2}$ ($Co^{III/II}$) of common cobalt porphyrin or non-macrocycle complexes investigated as homogeneous ORR catalysts (−0.10 V to +0.39 V vs Fc^{*+}/Fc*) that are selective for H_2O_2 production.[3]

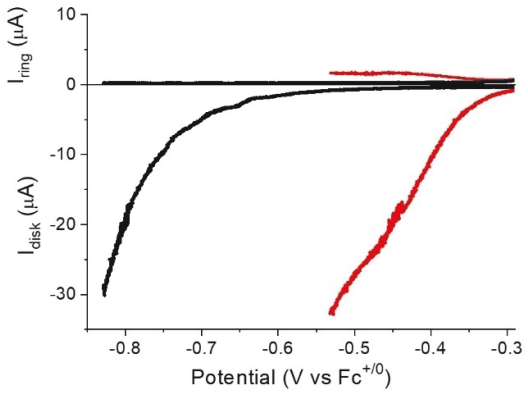

Figure 3. The rotating ring-disk electrode voltammograms (RRDEV) of a 15.0 mM $LutH^+$ + 15.0 mM Lut MeCN solution in the absence (black line) or presence (red line) of 0.1 mM $\mathbf{Co_2}^{\mathbf{SS}}$ under an oxygen-saturated atmosphere. Supporting electrolyte: 0.1 M *n*-Bu_4NPF_4 in MeCN, scan rate: 5 mV s^{-1}, rotation rate 1500 rpm. The disk current was recorded with a GC disk. The ring current was recorded with a Pt ring held at 0.2 V vs Fc^+/Fc.

Comparison with literature. We have previously demonstrated that dinuclear thiolate-based Fe and Mn complexes ($\mathbf{M_2}^{\mathbf{SH}}$, M = Fe, Mn) can be exploited as stable and efficient ORR catalysts.[12] While both catalysts exhibited selectivity for generating H_2O_2 in the presence of a chemical reducing agent (94(±4)% and 82(±2)% for the Fe and Mn catalysts, respectively), the selectivity of the Fe-complex shifted to the production of H_2O under electro-assisted conditions (<98%). Under chemical catalysis, $\mathbf{Fe_2}^{\mathbf{SH}}$ also displayed a faster kinetics compared to $\mathbf{Mn_2}^{\mathbf{SH}}$ (TOFi = 8 (±1) ×10^3 h^{-1} vs TOFi = 4.0 (±0.4) ×10^2 h^{-1}, respectively). In this study, we evidenced a significant difference in selectivity with the parent Co-based catalyst $\mathbf{Co_2}^{\mathbf{SS}}$, which favors the $4H^+/4e^-$ ORR process even in the presence of a chemical-reductant while maintaining comparable kinetics (TOFi = 3(±0.5) ×10^3 h^{-1}) with respect to $\mathbf{Fe_2}^{\mathbf{SH}}$.

In the case of the Mn and Fe parent complexes, DFT calculations suggest that dinuclear bridging peroxo M^{III} complexes serve as the key intermediate species. Upon comparing data from the Machan group on a mononuclear Co complex,[5] where the N2O2-donor supporting ligand still includes a bipyridine unit but is substituted by two phenols instead of alkyl thiolates, we propose, in the present case, a similar peroxo intermediate with a terminally bound Co^{III}-hydroperoxo species ($\mathbf{Co}^{\mathbf{OOH}}$ in Scheme 1). Unfortunately, despite multiple attempts, we were unable to detect this species. This difference in nuclearity for the key peroxo intermediate between the Mn/Fe and Co ORR catalysts may explain the opposite selectivity observed under chemical catalysis. Under these conditions, mononuclear peroxo complexes appear to preferentially facilitate O–O bond breaking, while dinuclear complexes exhibit a propensity for M–O bond rupture.

In a broader context of molecular Co-based ORR catalysts, the present system is unique for its thiolate ligation and stands out as one of the rare selective Co complexes promoting $4H^+/4e^-$ ORR catalysis. Typically, N4-macrocycle Co-based catalysts are known for their capacity to selectively convert O_2 into H_2O_2.[17] Only a few examples have been reported where the selectivity has been turned to H_2O either by adjusting experimental conditions or by modifying the second coordination sphere.[18] Shifting to non-macrocycle-based complexes with several N_xO_y environments in the first coordination sphere has enabled a shift from H_2O_2[3,17d] to H_2O[4–5,7] production. It is difficult to compare the respective performance of these systems quantitatively because of different experimental conditions, especially regarding the proton sources. However, with respect to other non-macrocycle Co-complexes selective for H_2O production, $\mathbf{Co_2}^{\mathbf{SS}}$ displays high performances, especially in

terms of overpotential and kinetics.[4b,5–, 6d] For instance, the parent Co catalyst reported by the Machan's group[5] is characterized by $\eta = 1.24$ V with a selectivity for H_2O of 71% and TOFi = 37 h^{-1} (for **Co_2^{SS}**: 0.81 V < η < 1.10 V, with a selectivity for H_2O of 93% and a TOFi = 3 000 h^{-1}).

Conclusions

The present study highlights the influence of the metal on the selectivity of the chemical ORR process, paralleling observations made in the context of the Co/Fe porphyrin-based ORR catalysts.[3] It also underscores the crucial role of the first coordination sphere. Indeed, with this N2S2 ligand, we noted an unusual trend: selectivity for $4H^+/4e^-$ ORR with Co and for $2H^+/2e^-$ ORR with Fe (under chemical catalysis). In contrast, Co-based porphyrins generally exhibit selectivity for H_2O_2, while the Fe-based ones favor the generation of H_2O.

Experimental Part

The compounds $[Co_2L^{SS}](PF_6)_2$,[11] and [CoL],[13] were prepared as previously described. Acetonitrile was distilled over CaH_2 and degassed prior to use. The electronic absorption spectra were recorded on a StarLine AvaSpec-ULS2048CL-EVO absorption photodiode-array spectrophotometer from Avantes in quartz cells (optical path length: 1 cm).

Chemical catalysis and detection of H_2O_2. The oxidation of Me_8Fc by O_2 in the presence of $[Co_2L^{SS}](PF_6)_2$ catalysts and 2,6-lutidinium tetrafluoroborate ($LutHBF_4$) was monitored in MeCN at 293 K by visible absorption spectroscopy. The catalytic results are summarized in Table S1. In a typical experiment, an air-saturated solution of $LutHBF_4$ (25 μL, 2.0 M) was added to an air-saturated solution of Me_8Fc (364 μL, 13.75 mM) in MeCN (1861 μL), in presence of air (1 atm, 0.21 atm O_2), in a septum-sealed 1 cm quartz cuvette kept at 293 K. After stirring for 5 s, an Ar-saturated solution of $[Co_2L^{SS}](PF_6)_2$ (250 μL, 1.0 mM) was added to the sample under stirring (air-saturated, 2.0 mM Me_8Fc, 15.0 mM $LutHBF_4$, 100 μM $[Co_2L^{SS}]^{2+}$). The increase in the absorbance of a band at 750 nm, corresponding to the formation of the Me_8Fc^+ ion, was monitored with time by using an Avantes photodiode-array spectrophotometer (see above, $\Delta t = 0.5$ or 1 s). The corresponding control experiments were performed in the same conditions by adding MeCN (250 μL) instead of catalyst solution. All the experiments were repeated 3 times, obtaining highly reproducible data (in the 5% range). The amount of produced hydrogen peroxide in all these samples was determined at 20 s, 240 s, and 600 s by spectroscopic titration with an acidic solution of $[TiO(tpypH_4)]^{4+}$ complex (Ti-TPyP reagent).[12a]

Electrochemical measurements and electrochemical ORR. Cyclic voltammetry experiments were conducted using a PGSTAT100N Metrohm-Autolab potentiostat/galvanostat in CH_3CN solution in an argon- or oxygen-saturated atmosphere. The supporting electrolyte tetrabutylammonium hexafluorophosphate (Bu_4NPF_6) was used as received and stored in a glove box. A standard three-electrode electrochemical cell was used. Potentials were referred to an Ag/0.01 M $AgNO_3$ reference electrode in CH_3CN + 0.1 M Bu_4NClO_4, and measured potentials were calibrated using an internal Fc/Fc^+ standard. The working electrode was a vitreous carbon disk (3 mm in diameter) polished with 2 μm diamond paste (Mecaprex Presi) (Ep_a, anodic peak potential; Ep_c, cathodic peak potential; $E_{1/2} = (Ep_a + Ep_c)/2$; $\Delta Ep = Ep_a - Ep_c$).

Rotating ring-disk electrode (RRDE) measurements were performed using a conventional three-electrode electrochemical cell setup connected to a bipotensiostat (Ametek) and a MSR rotator (Pine Instruments). Pine rotating ring-disk electrode is composed of a glassy carbon (GC) disk (0.196 cm2) and a Pt ring (0.11 cm2). The counter electrodes consisted of a Pt wire, and the reference electrode consisted of a saturated calomel electrode (SCE). RRDE experiments were carried out in MeCN (0.1 M Bu_4NPF_6) solution under Ar- and O_2-saturated atmosphere. Polarization curves were recorded at 5 mV s^{-1} (the response does not change within the range 2–10 mV s^{-1}), with 1500 rpm rotation speed. The potential of the Pt ring was set at 0.2 V and 0.43 V vs Fc^+/Fc to detect H_2O_2, while it was set at 0 V vs Fc^+/Fc to estimate the corresponding "blank".

All potentials were converted vs Fc^+/Fc. The SCE reference electrode was calibrated with the internal Fc^+/Fc reference system, which was found at + 0.40 V vs SCE. The Fc^+/Fc couple (E^0Fc^+/Fc = 0.53 V vs NHE, taking into account interliquid junction potential) could be further used to convert potentials vs NHE. The SCE reference electrode was also calibrated with the $[Fe(CN)_6]^{3-}/[Fe(CN)_6]^{4-}$ couple in an external electrochemical setup. Calibration against the $[Fe(CN)_6]^{3-}/[Fe(CN)_6]^{4-}$ couple was performed with a glassy carbon electrode and a platinum wire as working and auxiliary electrodes, respectively, in 0.1 M potassium phosphate buffer (pH = 7). The potential of the $[Fe(CN)_6]^{3-}/[Fe(CN)_6]^{4-}$ couple is denoted below as $E_{Fe(III)/Fe(II)}$ (0.185 V vs SCE) and $E_{Fe(III)/Fe(II)}$ vs NHE (0.425 V) refers to the tabulated value of $E_{Fe(III)/Fe(II)}$ against the NHE potential.

The faradaic efficiency for H_2O_2 production as a function of the potential applied at the disk is obtained according to equation (S1). The equation (S2) was used to calculate n.

$$(S1)\%H_2O_2 = \frac{2I_r(E)/N}{I_d(E) + I_r(E)/N} \times 100$$

$$(S2)n = \frac{4I_d(E)}{(I_d(E) + (I_r(E)/N))}$$

where Ir(E) and Id(E) are the absolute values of ring and disk current at potential E, and N is the collection efficiency of the electrode. The value of N was determined to be 0.265 using the one-electron $[Fe(CN)_6]^{3-/4-}$ redox couple.

ESI-mass experiments. Low-resolution electrospray ionization (ESI) mass spectra were recorded using an LCMS8060 triple-quadrupole mass spectrometer (Shimadzu Corporation, Kyoto, Japan) in positive ionization mode by direct infusion in the ESI source. Mass spectra data were acquired using *LabSolutions* software (version 5.114, Shimadzu Corporation, Kyoto, Japan). Desolvated ions were obtained using a capillary voltage at 3.5 kV, a source temperature of 100 °C, and nitrogen as the desolvation and nebulizing gas. Solutions were injected at a concentration of $2{\cdot}10^{-4}$ M into the ion source using a syringe pump at a flow rate of 1 mL/hr. The high-resolution mass spectra were recorded on an LTQ Orbitrap XL Thermo Scientific spectrometer equipped with an ESI source. Solutions were injected at a concentration of $4.5{\cdot}10^{-4}$ M into the ion source using a syringe pump at a flow rate of 5 μL/min.

Acknowledgements

The authors gratefully acknowledge research support of this work by the China Scholarship Council (LS), the French National Agency for Research in the framework of the "Investissements d'avenir" program (ANR-15-IDEX-02), the Labex ARCANE, CBH-EUR-GS (ANR-17-EURE-0003), and also the PRC program, SelectO2 (ANR-22-CE07-0045). T.A.J. acknowledges support from the US NSF from CHE-2154955 and CHE-1900384. Yannig Nedellec is gratefully acknowledged for RRDE experiments.

Conflict of Interests

The authors declare no conflict of interest.

Data Availability Statement

The data that support the findings of this study are available from the corresponding author upon reasonable request.

Keywords: dioxygen reduction · cobalt complex · electrocatalysis · homogeneous catalysis · inorganic chemistry · redox chemistry · thiolate ligand

[1] a) I. Yamanaka, T. Murayama, *Angew. Chem. Int. Ed.* **2008**, *47*, 1900–1902; b) R. S. Disselkamp, *Int. J. Hydrogen Energy* **2010**, *35*, 1049–1053; c) A. E. Sanli, A. Aytaç, *Int. J. Hydrogen Energy* **2011**, *36*, 869–875.
[2] a) M. K. Awasthi, A. Saini, C. Das, A. Banerjee, N. A. Shah, G. K. Lahiri, A. Dutta, *Eur. J. Inorg. Chem.* **2023**, *26*, e202300204; b) A. Boudghene Stambouli, E. Traversa, *Renewable Sustainable Energy Rev.* **2002**, *6*, 295–304; c) N. M. Marković, T. J. Schmidt, V. Stamenković, P. N. Ross, *Fuel Cells* **2001**, *1*, 105–116.
[3] a) Y.-H. Wang, B. Mondal, S. S. Stahl, *ACS Catal.* **2020**, *10*, 12031–12039; b) Y.-H. Wang, M. L. Pegis, J. M. Mayer, S. S. Stahl, *J. Am. Chem. Soc.* **2017**, *139*, 16458–16461.
[4] a) S. V. Obisesan, C. Rose, B. H. Farnum, C. R. Goldsmith, *J. Am. Chem. Soc.* **2022**, *144*, 22826–22830; b) A. Das, A. Ali, G. Gupta, A. Santra, P. Jain, P. P. Ingole, S. Paul, S. Paria, *ACS Catal.* **2023**, *13*, 5285–5297.
[5] A. W. Nichols, J. S. Kuehner, B. L. Huffman, P. R. Miedaner, D. A. Dickie, C. W. Machan, *Chem. Commun.* **2021**, *57*, 516–519.
[6] a) H. Arima, M. Wada, T. Nakazono, T. Wada, *Inorg. Chem.* **2021**, *60*, 9402–9415; b) G. Passard, A. M. Ullman, C. N. Brodsky, D. G. Nocera, *J. Am. Chem. Soc.* **2016**, *138*, 2925–2928; c) T. Wada, H. Maki, T. Imamoto, H. Yuki, Y. Miyazato, *Chem. Commun.* **2013**, *49*, 4394–4396; d) S. Fukuzumi, S. Mandal, K. Mase, K. Ohkubo, H. Park, J. Benet-Buchholz, W. Nam, A. Llobet, *J. Am. Chem. Soc.* **2012**, *134*, 9906–9909.
[7] I. Monte-Pérez, S. Kundu, A. Chandra, K. E. Craigo, P. Chernev, U. Kuhlmann, H. Dau, P. Hildebrandt, C. Greco, C. Van Stappen, N. Lehnert, K. Ray, *J. Am. Chem. Soc.* **2017**, *139*, 15033–15042.
[8] a) P. Kumar, L. Devkota, M. C. Casey, A. A. Fischer, S. V. Lindeman, A. T. Fiedler, *Inorg. Chem.* **2022**, *61*, 16664–16677; b) P. Kumar, S. V. Lindeman, A. T. Fiedler, *J. Am. Chem. Soc.* **2019**, *141*, 10984–10987.
[9] J. B. Gordon, A. C. Vilbert, I. M. DiMucci, S. N. MacMillan, K. M. Lancaster, P. Moënne-Loccoz, D. P. Goldberg, *J. Am. Chem. Soc.* **2019**, *141*, 17533–17547.
[10] B. Battistella, L. Iffland-Mühlhaus, M. Schütze, B. Cula, U. Kuhlmann, H. Dau, P. Hildebrandt, T. Lohmiller, S. Mebs, U.-P. Apfel, K. Ray, *Angew. Chem. Int. Ed.* **2023**, *62*, e202214074.
[11] M. Gennari, B. Gerey, N. Hall, J. Pécaut, M.-N. Collomb, M. Rouzières, R. Clérac, M. Orio, C. Duboc, *Angew. Chem. Int. Ed.* **2014**, *53*, 5318–5321.
[12] a) L. Wang, M. Gennari, F. G. Cantú Reinhard, J. Gutiérrez, A. Morozan, C. Philouze, S. Demeshko, V. Artero, F. Meyer, S. P. de Visser, C. Duboc, *J. Am. Chem. Soc.* **2019**, *141*, 8244–8253; b) M. Gennari, D. Brazzolotto, J. Pecaut, M. V. Cherrier, C. J. Pollock, S. DeBeer, M. Retegan, D. A. Pantazis, F. Neese, M. Rouzieres, R. Clerac, C. Duboc, *J. Am. Chem. Soc.* **2015**, *137*, 8644–8653.
[13] M. Gennari, B. Gerey, N. Hall, J. Pécaut, H. Vezin, M. N. Collomb, M. Orio, C. Duboc, *Dalton Trans.* **2012**, *41*, 12586–12594.
[14] L. K. Wang, F. G. C. Reinhard, C. Philouze, S. Demeshko, S. P. de Visser, F. Meyer, M. Gennari, C. Duboc, *Chem. Eur. J.* **2018**, *24*, 11973–11982.
[15] H. Noh, J. M. Mayer, *Chem* **2022**, *8*, 3324–3345.
[16] E. N. Cook, D. A. Dickie, C. W. Machan, *J. Am. Chem. Soc.* **2021**, *143*, 16411–16418.
[17] a) M. L. Pegis, C. F. Wise, D. J. Martin, J. M. Mayer, *Chem. Rev.* **2018**, *118*, 2340–2391; b) C. W. Machan, *ACS Catal.* **2020**, *10*, 2640–2655; c) Y. Li, N. Wang, H. Lei, X. Li, H. Zheng, H. Wang, W. Zhang, R. Cao, *Coord. Chem. Rev.* **2021**, *442*, 213996; d) A. W. Nichols, E. N. Cook, Y. J. Gan, P. R. Miedaner, J. M. Dressel, D. A. Dickie, H. S. Shafaat, C. W. Machan, *J. Am. Chem. Soc.* **2021**, *143*, 13065–13073; e) R. Zheng, Q. Meng, L. Zhang, J. Ge, C. Liu, W. Xing, M. Xiao, *Chem. Eur. J.* **2023**, *29*, e202203180.
[18] Y.-H. Wang, P. E. Schneider, Z. K. Goldsmith, B. Mondal, S. Hammes-Schiffer, S. S. Stahl, *ACS Cent. Sci.* **2019**, *5*, 1024–1034.

Manuscript received: February 7, 2024
Revised manuscript received: April 1, 2024
Accepted manuscript online: April 3, 2024
Version of record online: ■■, ■■